

Supplementary Information

Highly crystalline and robust covalent organic framework membranes for predictable solvent transport and molecular separation

Hukang Guo ^{a, b}, Jianxiao Jiang ^{a, b}, Chuanjie Fang ^{a, b, *}, Liping Zhu ^{a, b, c, *}

^a *MOE Key Laboratory of Macromolecular Synthesis and Functionalization,
Department of Polymer Science and Engineering, Zhejiang University, Hangzhou
310058, P.R. China*

^b *MOE Engineering Research Center of Membrane and Water Treatment Technology,
Zhejiang University, Hangzhou 310058, P.R. China*

^c *Center for Healthcare Materials, Shaoxing Institute, Zhejiang University, Shaoxing
312000, P.R. China*

* Corresponding author

Dr. Fang, fangchuanjie@zju.edu.cn

Prof. Zhu, lpzhu@zju.edu.cn

| | |
|------------------------------------|-----------|
| 1. Supporting Figures | 3 |
| 2. Supporting Tables | 14 |
| 3. References..... | 16 |

1. Figures

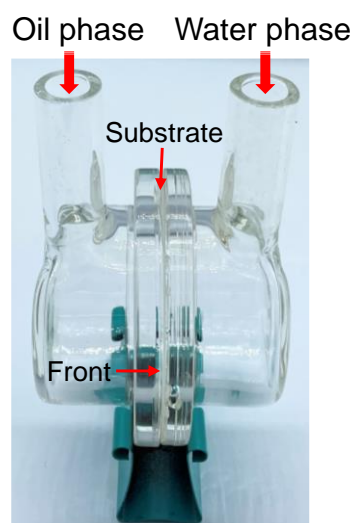


Fig. S1. Digital photograph of a homemade diffusion cell used for the growth of a COF-DT layer on a PAN support via interface polymerization.

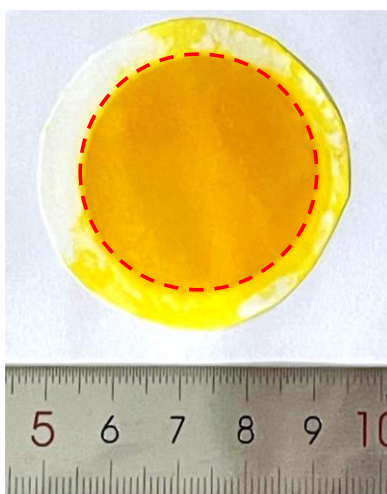


Fig. S2. Digital photograph of the COF-DT-2.7/PAN membrane.

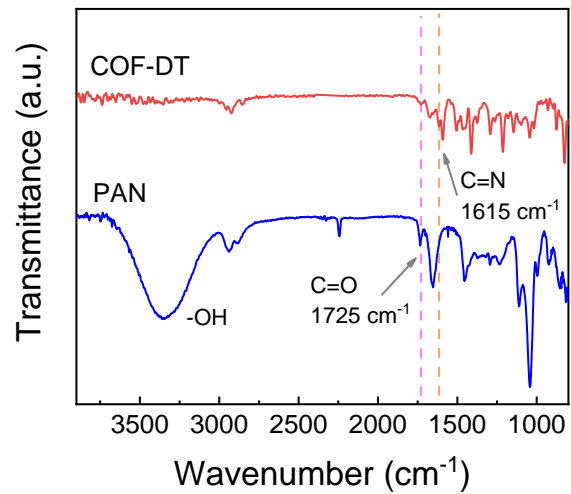


Fig. S3. ATR-FTIR spectra of the COF-DT/PAN and pristine PAN membranes.

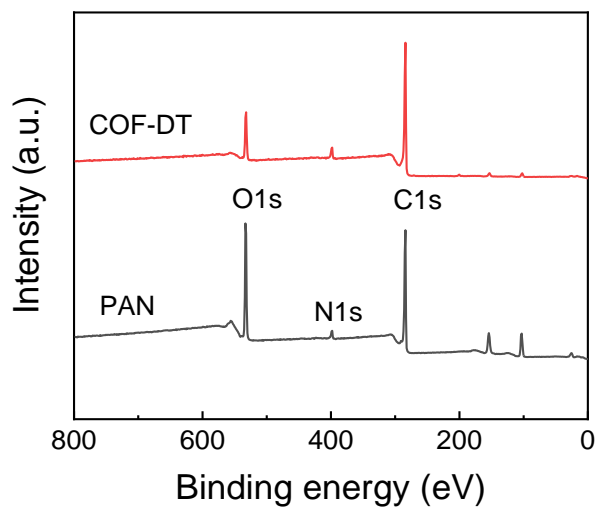


Fig. S4. XPS spectra of the COF-DT/PAN and pristine PAN membranes.

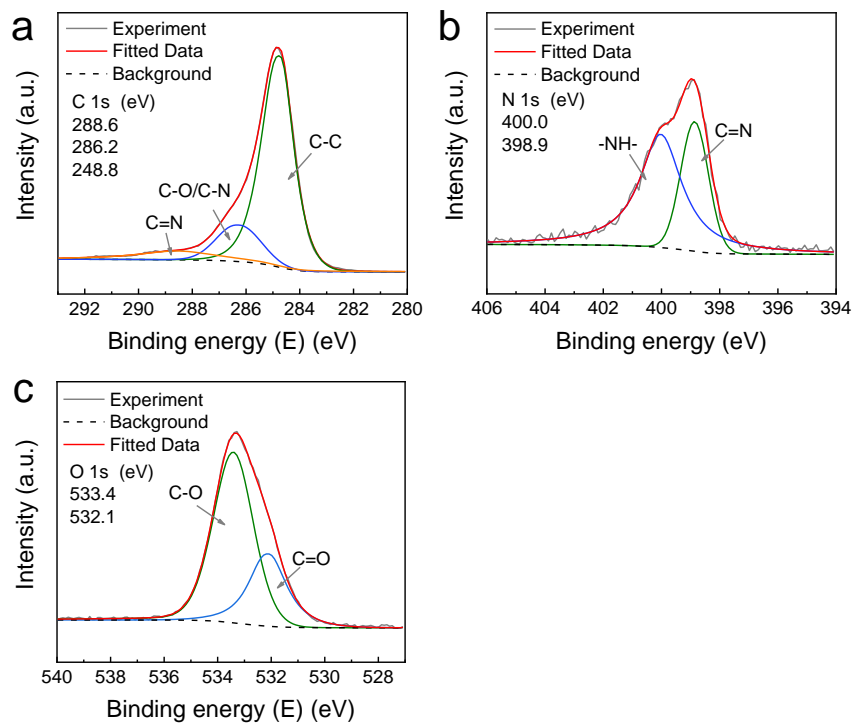


Fig. S5. High-resolution XPS spectra of C 1s (a), N 1s (b), and O 1s (c) for the COF-DT/PAN membrane.

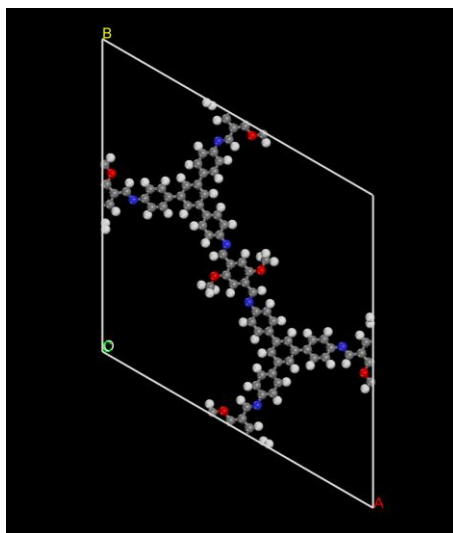


Fig. S6. Unit cell of the AA stacking mode of the COF-DT (O, red; N, blue; C, grey).

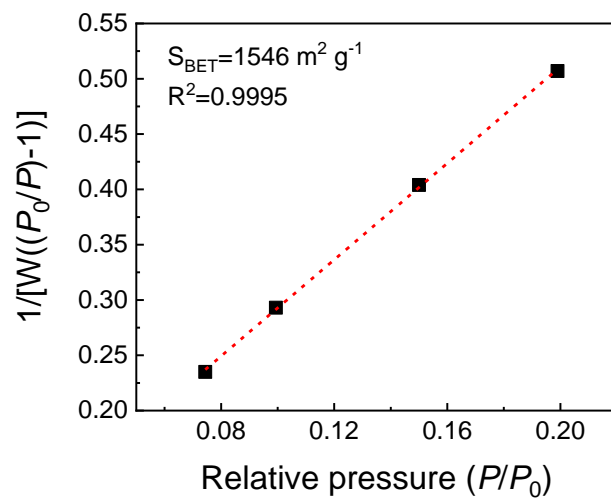


Fig. S7. BET plot calculated from the N₂ adsorption isotherm.

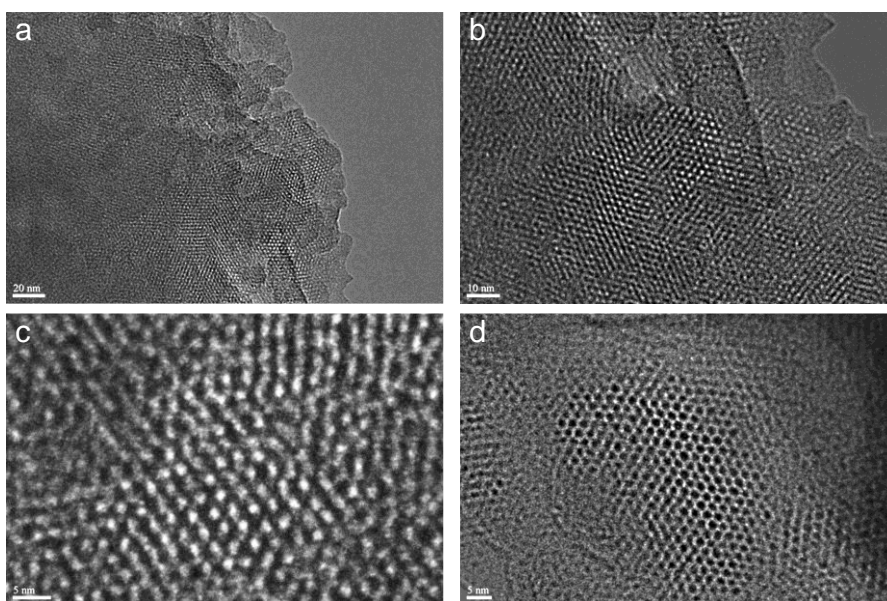


Fig. S8. HRTEM images of the COF-DT-2.7 film under different magnifications.

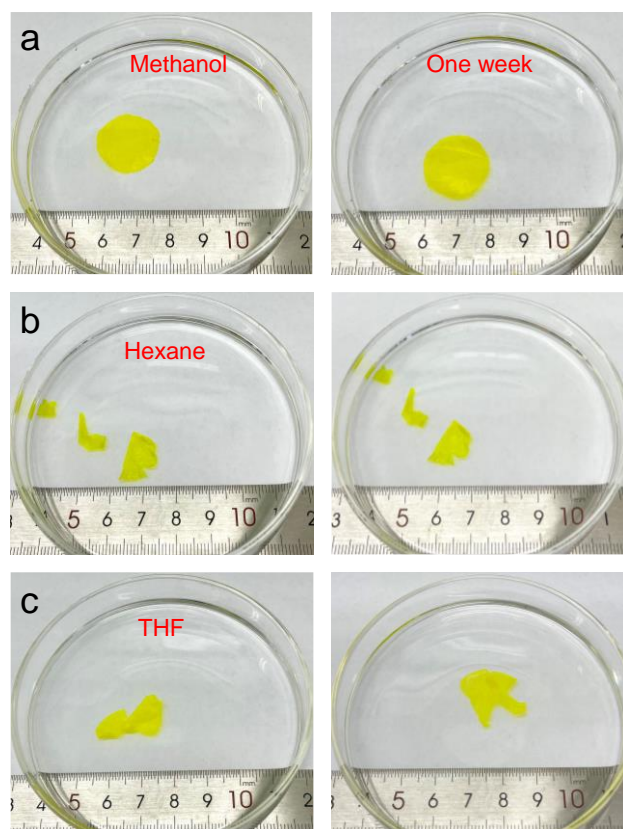


Fig. S9. Digital photographs of COF-DT-2.7 films before and after treatment for one week in methanol (a), hexane (b), and THF (c).

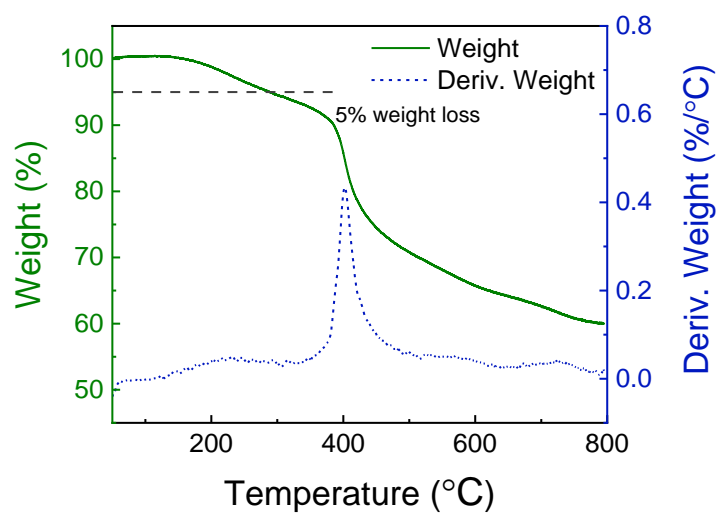


Fig. S10. TGA and DTG curves of the COF-DT-2.7 film under N₂.

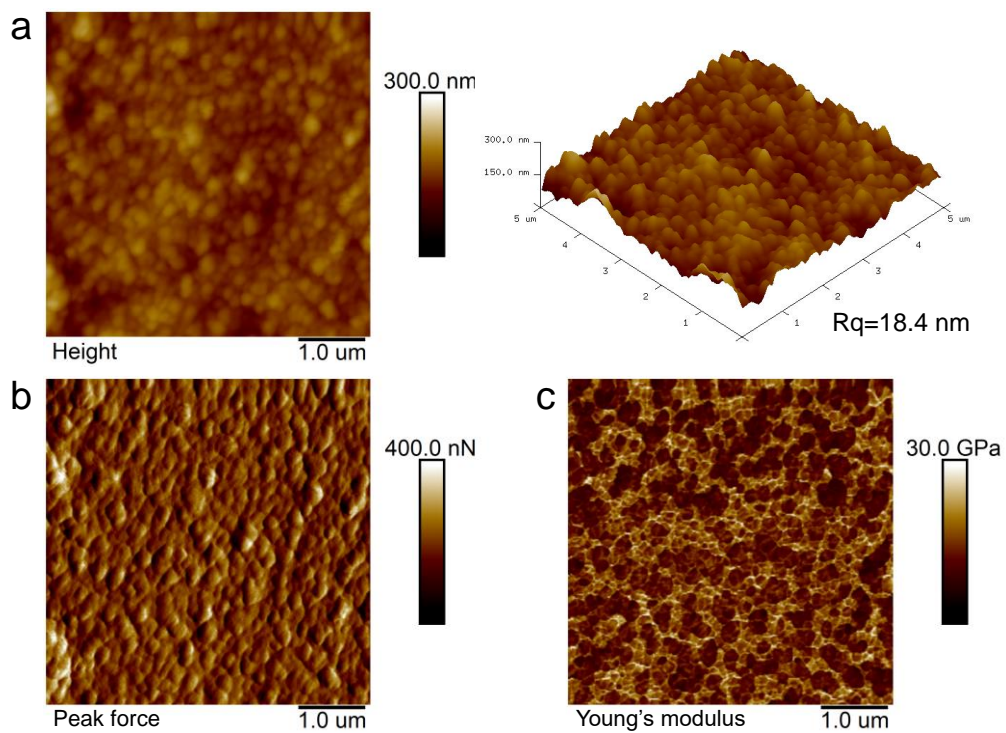


Fig. S11. AFM images of the COF-DT-2.7 film measured by height (a), peak force (b), and Young's modulus (c) modes.

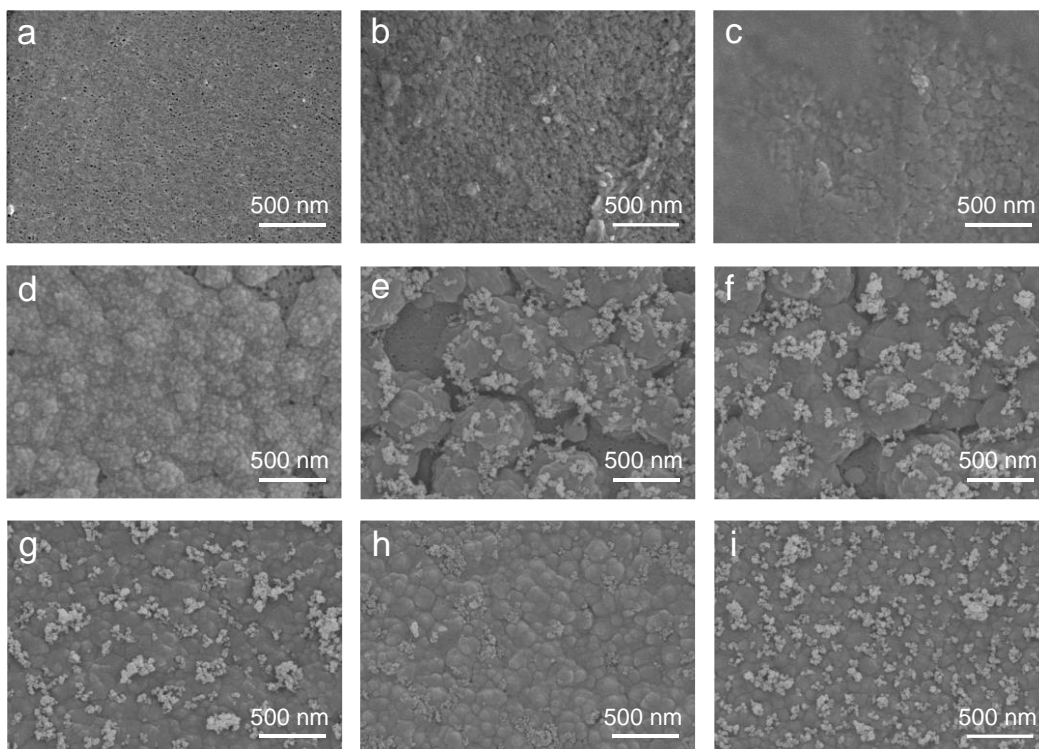


Fig. S12. Surface SEM images of the PAN (a), COF-DT-0.9/PAN (b), COF-DT-1.2/PAN (c), COF-DT-1.5/PAN (d), COF-DT-1.8/PAN (e), COF-DT-2.1/PAN (f), COF-DT-2.4/PAN (g), COF-DT-2.7/PAN (h), COF-DT-3.0/PAN (i) membranes.

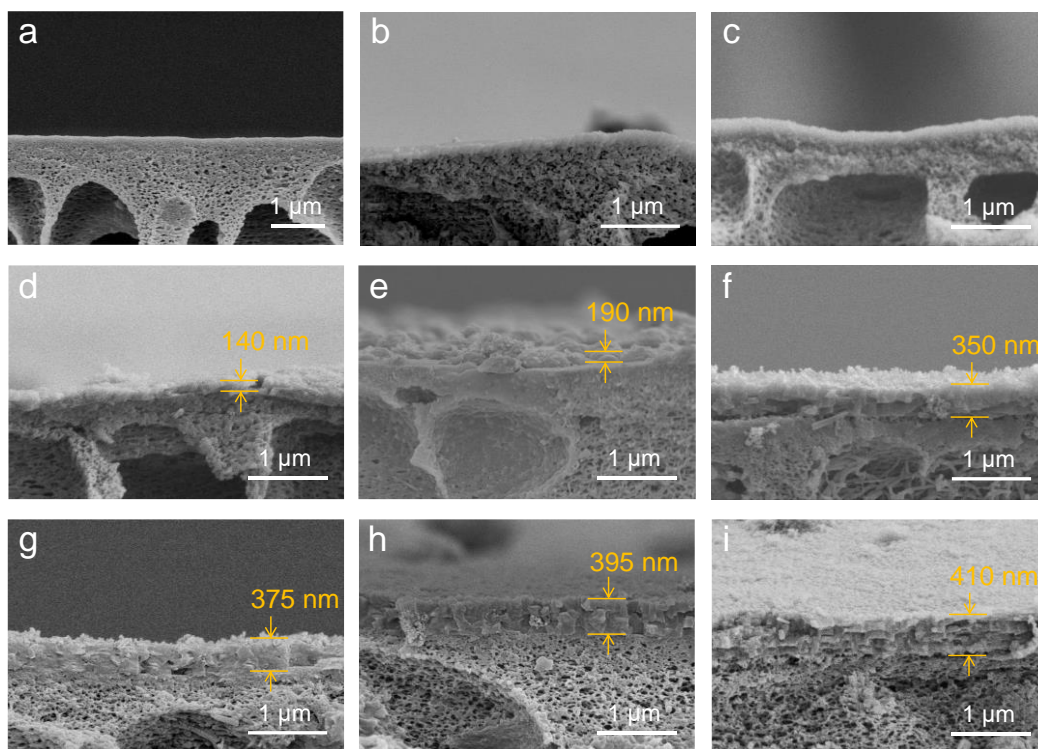


Fig. S13. Cross-section SEM images of the PAN (a), COF-DT-0.9/PAN (b), COF-DT-1.2/PAN (c), COF-DT-1.5/PAN (d), COF-DT-1.8/PAN (e), COF-DT-2.1/PAN (f), COF-DT-2.4/PAN (g), COF-DT-2.7/PAN (h), COF-DT-3.0/PAN (i) membranes.

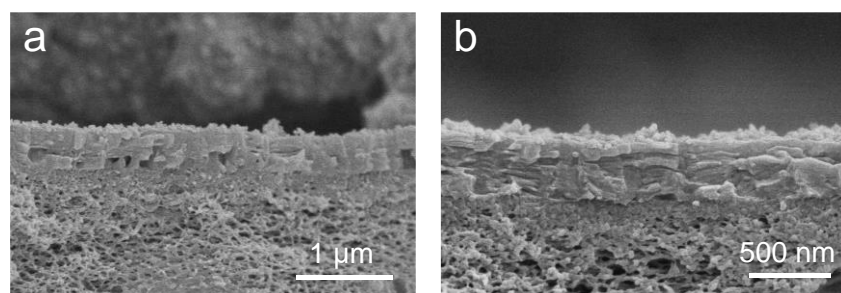


Fig. S14. Cross-section SEM images of the COF-DT-3.0/PAN membrane with different magnification factors.

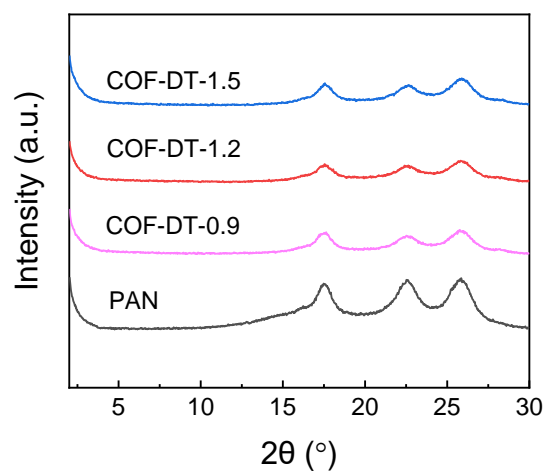


Fig. S15. XRD patterns of various COF-DT/PAN membranes prepared using different TAPB concentrations.

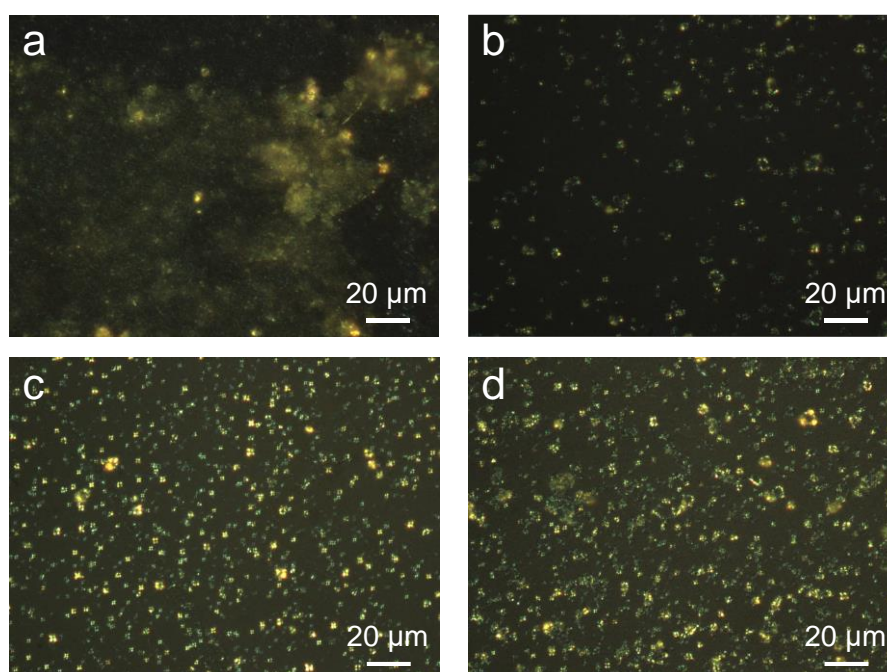


Fig. S16. Microscopic images of the COF-DT-2.1 (a), COF-DT-2.4 (b), COF-DT-2.7 (c), COF-DT-3.0 (d) films.

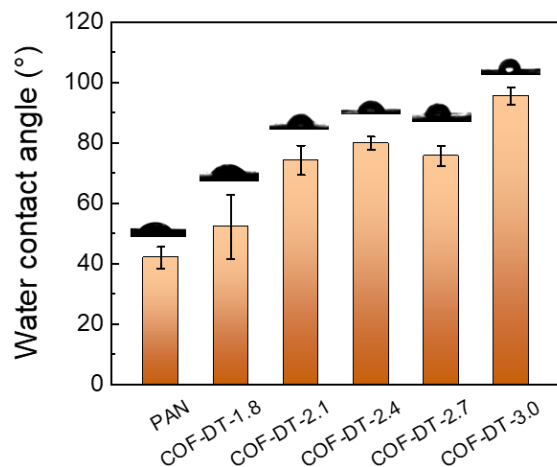


Fig. S17. Water contact angles of the PAN (a), COF-DT-1.8/PAN (b), COF-DT-2.1/PAN (c), COF-DT-2.4/PAN (d), COF-DT-2.7/PAN (e), COF-DT-3.0/PAN (f) membranes.

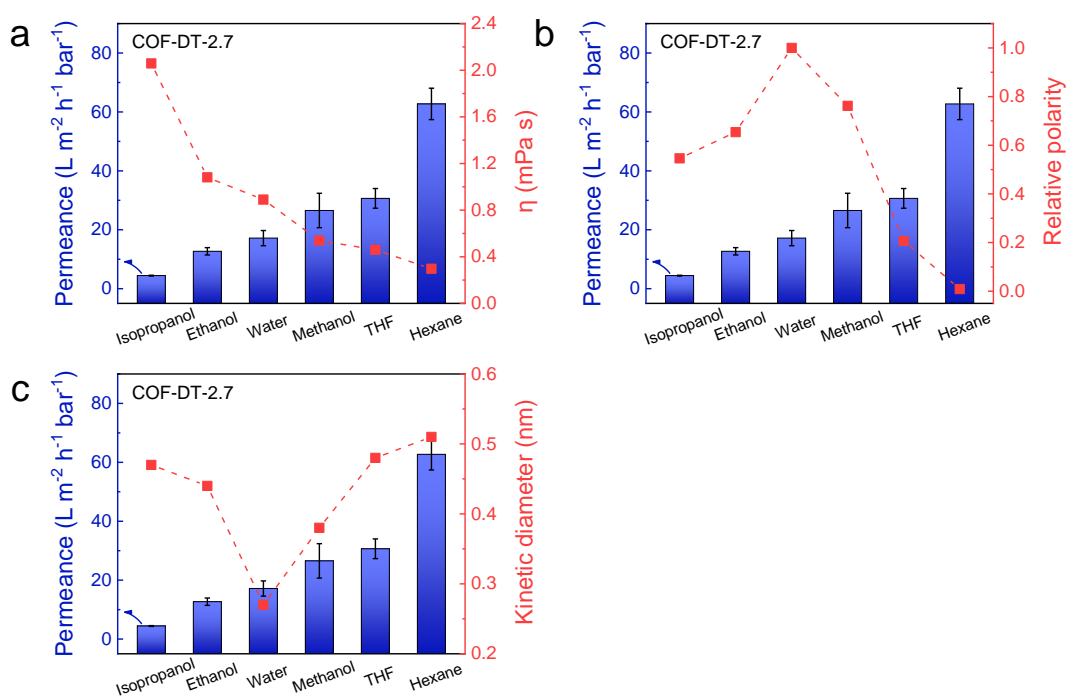


Fig. S18. The plots of solvent viscosity (a), relative polarity (b), and kinetic diameter (c) versus solvent permeance through the COF-DT-2.7/PAN membrane.

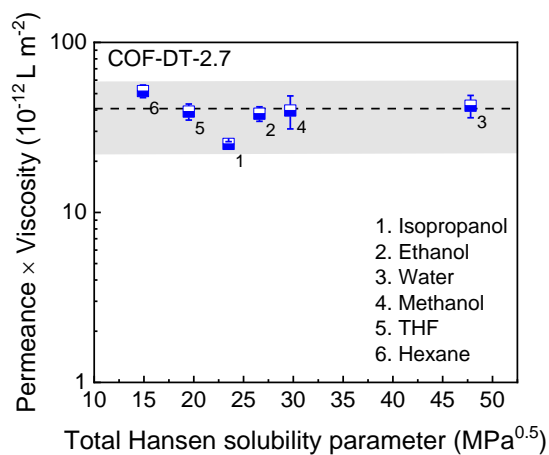


Fig. S19. Product of solvent permeance and viscosity as a function of the total Hansen solubility parameter for the COF-DT-2.7/PAN membrane.

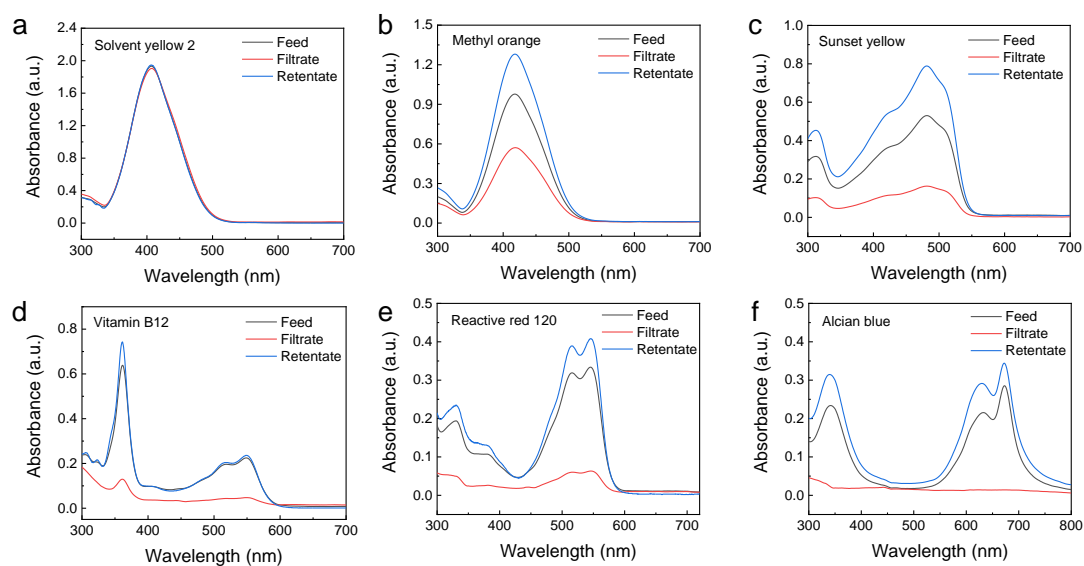


Fig. S20. UV-vis absorption spectra of various dye solution in ethanol (20 ppm) before and after filtration through the COF-DT-2.7/PAN membrane.

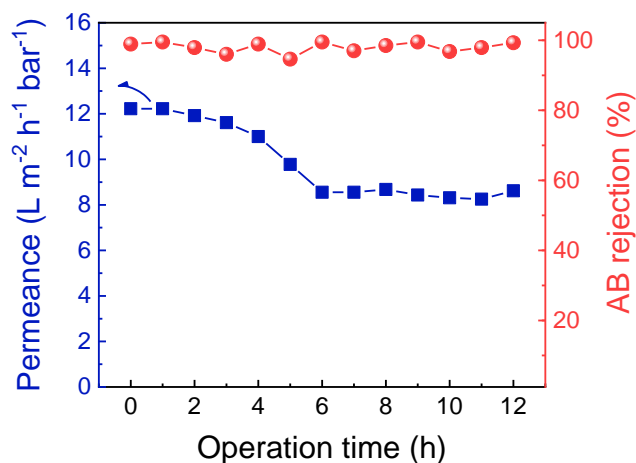
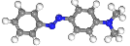
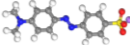
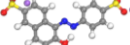
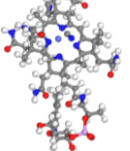
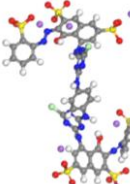


Fig. S21. Long-term separation stability of the COF-DT-2.7/PAN membrane toward the ethanolic AB solution in a crossflow filtration under 4 bar.

2. Tables

Table S1. Detailed properties of different dye molecules used in this work.

| Dye | Structure | Molecular size (Å) | Molecular weight (g/mol) | Charge | UV-vis absorption peak (nm) |
|------------------|-------------------------------------------------------------------------------------|--------------------|--------------------------|--------|-----------------------------|
| Solvent yellow 2 |  | 15.7×7.0×4.1 | 225.29 | 0 | 408 |
| Methyl orange |  | 18.6×7.4×6.6 | 327.33 | – | 420 |
| Sunset yellow |  | 19.7×9.8×7.1 | 452.36 | – | 482 |
| Vitamin B12 |  | 22.6×17.1×7.0 | 1355.38 | 0 | 362 |
| Reactive red 120 |  | 25.3×17.2×12.4 | 1469.98 | – | 545 |

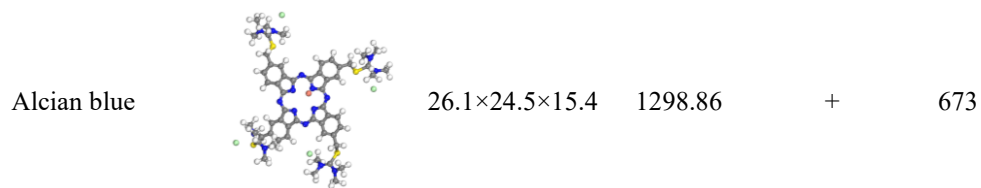


Table S2. Element compositions of membranes.

| Membranes | C (%) | N (%) | O (%) |
|-----------|-------|-------|-------|
| PAN | 66.8 | 3.9 | 29.3 |
| COF-DT | 80.4 | 5.5 | 14.1 |

Table S3. Solvent properties.

| Solvent | Viscosity at 25 °C (mPa s) ¹ | Relative polarity ^{2,3} | Kinetic diameter (nm) ^{1,4} | Total solubility (MPa ^{0.5}) ¹ | Hansen parameter |
|-------------|--------------------------------------------|----------------------------------|-----------------------------------------|--------------------------------------------------------|---------------------|
| Isopropanol | 2.06 | 0.546 | 0.47 | 23.5 | |
| Ethanol | 1.08 | 0.654 | 0.44 | 26.6 | |
| Water | 0.92 | 1 | 0.27 | 47.8 | |
| Methanol | 0.54 | 0.762 | 0.38 | 29.7 | |
| THF | 0.46 | 0.207 | 0.48 | 19.5 | |
| Hexane | 0.29 | 0.009 | 0.51 | 14.9 | |

3. References

1. A. Buekenhoudt, F. Bisignano, G. De Luca, P. Vandezande, M. Wouters and K. Verhulst, *J. Membr. Sci.*, 2013, **439**, 36-47.
2. Q. Yang, Y. Su, C. Chi, C. T. Cherian, K. Huang, V. G. Kravets, F. C. Wang, J. C. Zhang, A. Pratt, A. N. Grigorenko, F. Guinea, A. K. Geim and R. R. Nair, *Nat. Mater.*, 2017, **16**, 1198-1202.
3. P. J. Linstrom and W. G. Mallard, *J. Chem. Eng. Data*, 2001, **46**, 1059-1063.
4. J. Liu, S. Wang, T. Huang, P. Manchanda, E. Abou-Hamad and S. P. Nunes, *Sci Adv*, 2020, **6**, eabb3188.